Breast Cancer: Targets and Therapy

Dovepress
Taylor & Francis Group

Open Access Full Text Article

ORIGINAL RESEARCH

Identification of Potential Therapeutic Targets for Xihuang Pill in Breast Cancer: A Mendelian Randomization and Experimental Study

Yuning Tang[1], Zhuotao Yang[1], Zhihao Ye[2], Haotian Su[3], Ruotong Zhu[4], Xuli Meng[2,*], Qinghui Zheng[2,*]

[1]The Second Clinical Medical College, Zhejiang Chinese Medical University, Hangzhou, Zhejiang, 310053, People's Republic of China; [2]Department of Breast Surgery, General Surgery, Cancer Center, Zhejiang Provincial People's Hospital (Affiliated People's Hospital), Hangzhou Medical College, Hangzhou, Zhejiang, 310053, People's Republic of China; [3]The Second School of Clinical Medicine, Hangzhou Normal University, Hangzhou, Zhejiang, 310053, People's Republic of China; [4]The First Clinical College of Zhejiang Chinese Medical University, Hangzhou, Zhejiang, 310053, People's Republic of China

*These authors contributed equally to this work

Correspondence: Xuli Meng; Qinghui Zheng, Department of Breast Surgery, General Surgery, Cancer Center, Zhejiang Provincial People's Hospital (Affiliated People's Hospital), Hangzhou Medical College, Hangzhou, Zhejiang, 310053, People's Republic of China, Email mxlmail@126.com; zhengqinghui@hmc.edu.cn

Purpose: Breast cancer remains a major threat to women's health worldwide, with drug resistance posing a significant challenge to treatment efficacy. Xihuang Pill (XHP), a traditional Chinese medicine formula, has demonstrated anti-tumor potential in breast cancer. However, its complex composition makes elucidating its precise molecular mechanisms difficult. This study aimed to identify key targets and mechanisms of XHP against breast cancer by integrating network pharmacology with Mendelian randomization analyses based on large-scale genome-wide association study (GWAS) and expression quantitative trait loci (eQTL) datasets, and thereby overcoming the subjectivity and uncertainty inherent in traditional target prediction.

Methods: Active ingredients and targets of XHP were retrieved from TCMSP and SymMap databases. Breast cancer risk-related genes were identified using summary-data-based MR (SMR) analysis integrating blood eQTL data from eQTLGen and GWAS data from FinnGen. Overlapping targets between XHP and breast cancer were analyzed. In vitro experiments, including siRNA knockdown and treatment with XHP-containing serum, were conducted on MCF-7 and MDA-MB-231 breast cancer cells to assess the roles of identified targets on cell proliferation (CCK-8 assay) and migration (wound healing assay), and to verify XHP's effects on target expression (Western blot, qRT-PCR).

Results: Network pharmacology identified 383 potential XHP targets. SMR analysis revealed 33 genes significantly associated with breast cancer risk. Intersection analysis pinpointed GSTM1 and SLC22A5 as overlapping targets. Notably, GSTM1 is a key enzyme involved in glutathione metabolism and cellular detoxification, whereas SLC22A5 (OCTN2) is a crucial transporter responsible for carnitine uptake and cellular energy metabolism. MR analysis indicated that higher expression of both genes was associated with reduced breast cancer risk. In vitro, silencing GSTM1 or SLC22A5 promoted proliferation and migration of breast cancer cells. Conversely, XHP-containing serum upregulated GSTM1 and SLC22A5 expression and significantly inhibited cancer cell proliferation and migration.

Conclusion: XHP may inhibit breast cancer cell proliferation and migration by upregulating GSTM1 and SLC22A5, offering new insights for precision TCM therapy.

Keywords: breast cancer, Xihuang pill, Mendelian randomization, GSTM1, SLC22A5

Introduction

Breast cancer (BC) is a heterogeneous disease related to both genetic and environmental factors. It is highly prevalent among women worldwide and poses a significant threat to women's health. According to the data released by the International Agency for Research on Cancer (IARC) in 2022, female breast cancer ranks as the second most prevalent

https://doi.org/10.2147/BCTT.S572244
Received: 9 October 2025
Accepted: 28 January 2026
Published: 6 February 2026

cancer globally, following lung cancer. In 2022, there were more than 2.3 million newly diagnosed breast cancer cases globally, accounting for 11.6% of the total number of newly diagnosed cancers. Additionally, there were more than 660,000 new deaths. Breast cancer is the most common malignant tumor among women and also the leading cause of cancer-related deaths in females.[1] Surgery remains the cornerstone of breast cancer treatment. Adjuvant systemic therapies, including postoperative chemotherapy, neoadjuvant chemotherapy (administered prior to surgery), radiotherapy, endocrine therapy, and targeted therapy, constitute the primary treatment modalities used in clinical practice.[2] Although a variety of treatment options have emerged in the past few decades to address the molecular diversity of breast cancer, the problem of drug resistance to endocrine drugs, chemotherapy drugs and targeted drugs remains a major obstacle in the treatment of breast cancer and an important adverse factor affecting the long-term prognosis of breast cancer patients.[3–6] Therefore, there is an urgent need to explore more safe, effective and widely applicable treatment modalities.

In traditional Chinese medicine (TCM), breast cancer is categorized under the pathological entity known as "Ruyan". The core therapeutic principle for managing this condition involves promoting blood circulation, resolving phlegm, and detoxifying to alleviate abscess formation. Xihuang Pill (XHP), a classical TCM formula with anti-tumor properties, was first documented in the Qing Dynasty text "Comprehensive Treatise on Surgical Diseases" by Wang Hongxu. Composed of four medicinal ingredients—bezoar, musk, myrrh, and frankincense—the formulation is traditionally employed for its heat-clearing, detoxifying, swelling-reducing, and nodule-dispersing effects.[7] In recent years, modern pharmacological studies have revealed that XHP contains a variety of key chemical constituents, such as boswellic acids, bile acids, bilirubin, muscone, and guggulsterones, which have been demonstrated to possess antitumor activities, collectively forming the modern pharmacological basis for its anti-cancer effects.[8,9] For instance, studies indicates that XHP may exert anti-tumor effects by inhibiting the proliferation, migration, invasion of breast cancer cells and the growth of transplanted tumors in vivo.[10] Network pharmacology studies have shown that XHP can regulate key targets of triple-negative breast cancer and potential important targets in the tumor microenvironment.[11] Therefore, applying XHP as an adjuvant treatment for breast cancer may have a positive effect on the prognosis of the disease. (It should be pointed out that the use of traditional Chinese medicine must be approved by medical authorities and can only be used as an adjunctive treatment, and must never replace the approved standard therapies). However, owing to the chemical complexity of traditional Chinese medicine and the intricate interactions between its components and the human biological system, elucidating their underlying molecular mechanisms remains a significant challenge. At present, network pharmacology has become the predominant approach for investigating TCM formulations. The identification of bioactive compounds and their potential action targets in TCM materials primarily relies on specialized databases such as TCMSP, BATMAN-TCM, and Symmap, whereas disease-related targets are predominantly sourced from public databases including Genecards, OMIM, and TTD.[12,13] This method exhibits a notable degree of subjectivity in the selection of drug and disease targets, frequently lacks standardized quantitative criteria, and the predictive validity of identified targets remains difficult to assess. More critically, it is often insufficiently supported by robust molecular biological evidence or experimentally validated data.[14]

Owing to the advancements in genome-wide association studies (GWAS), Mendelian randomization (MR) has emerged as a robust epidemiological tool for inferring causal relationships between exposures and outcomes.[15] Given that genetic variations are randomly allocated at the moment of conception, in contrast to observational studies, this approach is less prone to being influenced by confounding factors and reverse causality biases. Moreover, it remains unaffected by the progression of diseases.[16] Expression quantitative trait loci (eQTLs) play a critical role in elucidating the genetic regulation of gene transcription, where single nucleotide polymorphisms (SNPs) serve as key regulatory elements. Integrating GWAS data with eQTL information enables the identification of target genes associated with risk variants through causal inference approaches.[17,18] Based on this principle, Mendelian randomization enables the identification of target genes that show a strong association with diseases, thereby offering a clear direction for elucidating the target profiles of traditional Chinese medicine compound prescriptions and effectively addressing the limitations of traditional network pharmacology, such as subjectivity and uncertainty in target identification.

In this study, breast cancer, as a heterogeneous disease, has significant differences in clinical symptoms and prognosis among different molecular subtypes.[19] Therefore, identifying strongly correlated targets is of great significance for

exploring the mechanism of drug action, developing new drugs, and improving the prognosis of breast cancer.[20] Therefore, this study combined Mendelian randomization and network pharmacology methods. Firstly, it used summary data-based Mendelian randomization (SMR) analysis to screen out potential target genes significantly associated with breast cancer risk. Then, it conducted an intersection analysis between these genes and the predicted target points of XHP through network pharmacology methods to identify the potential action targets of XHP in treating breast cancer. Finally, in vitro experiments were carried out to verify the screening results, providing new empirical evidence for clarifying the mechanism of XHP in treating breast cancer. Based on the above rationale, we hypothesized that by integrating Mendelian randomization (which provides genetic-level causal evidence) with network pharmacology (which maps drug-target interactions), we could more reliably identify the key therapeutic targets of XHP against breast cancer, and subsequently validate their biological functions through experimentation. To test this hypothesis, we designed the study workflow illustrated in Figure 1.

Materials and Methods

Collect the Active Components and Action Targets of XHP

The active pharmacological ingredients of the four medicinal components—Bovis Calculus Biliaris, Moschus, Boswellia carterii, and Commiphora myrrha—comprising the XHP were systematically retrieved from the Traditional Chinese Medicine Systems Pharmacology database (TCMSP, https://www.tcmsp-e.com/index.php) and the SymMap database (http://www.symmap.org).[21,22] The screening criteria were defined as oral bioavailability (OB ≥ 30%) and drug-likeness (DL ≥ 0.18).[23] OB refers to the relative proportion or degree to which a drug can be absorbed and enter the systemic circulation after being administered orally.[24] DL serves as a fundamental tool in medicinal and computational chemistry, facilitating the prediction of complex biological systems and guiding early-stage drug discovery.[25] All target proteins associated with the active ingredients were mapped to their corresponding gene identifiers using the UniProt database

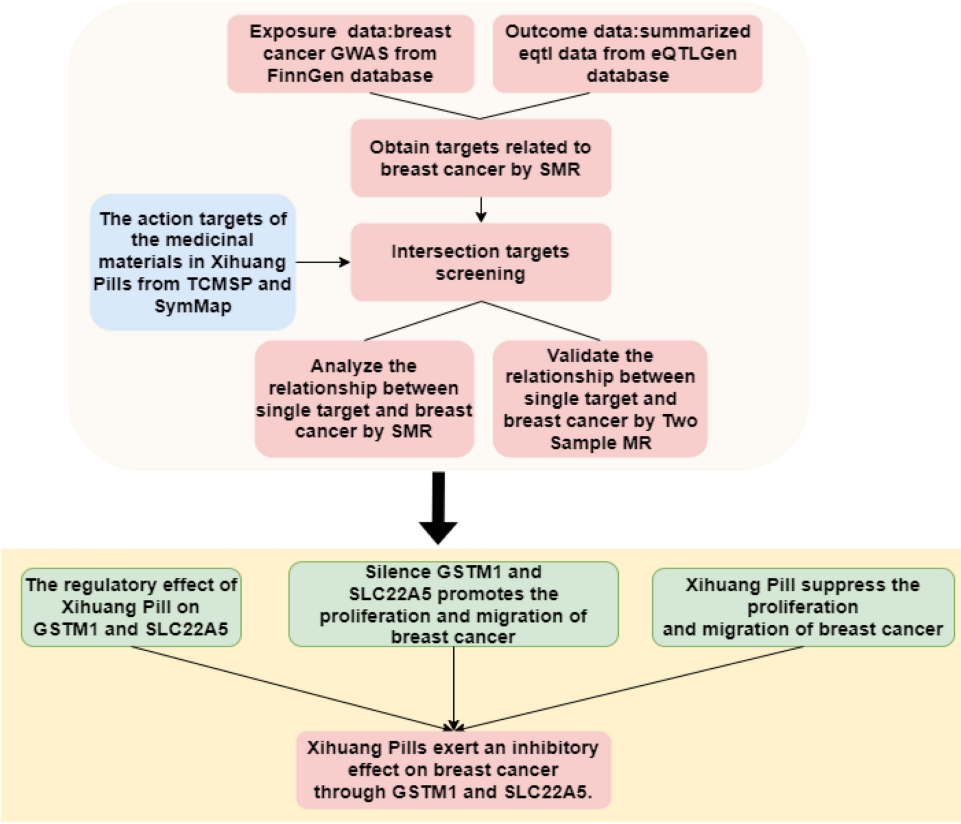

Figure 1 Flowchart.

https://doi.org/10.2147/BCTT.S572244

(https://www.uniprot.org/), with the species restricted to "Homo sapiens" to ensure human-specific target-gene associations.[26]

GO&KEGG Analyses

To systematically elucidate the potential mechanisms of action of Xihuang Pill, Gene Ontology (GO) and Kyoto Encyclopedia of Genes and Genomes (KEGG) pathway enrichment analyses were performed in R (version 4.2.1). The R packages clusterProfiler (version 4.4.4) and ggplot2 (version 3.4.4) were used for GO and KEGG enrichment analysis and result visualization, respectively. The significance of enrichment results was adjusted using the False Discovery Rate (FDR) method, with an adjusted p-value (p_{adj}) < 0.05 set as the statistically significant threshold.

Identification of Disease-Related Targets for Breast Cancer

eQTLs can reveal the relationship between SNPs and gene expression levels. The aggregated blood-based eQTL dataset used in this study was sourced from the eQTLGen consortium (https://www.eqtlgen.org/), encompassing a total of 31,684 samples.[27] The GWAS data on breast cancer outcomes were sourced from the FinnGen database (R12, https://www.finngen.fi/en).[28] The FinnGen Study is a large-scale project that encompasses both genotypic and clinical data, with up to 377,277 participants registered.[28] In this study, we utilized the SMR (v1.3.1) tool to conduct SMR analysis and HEIDI tests to assess the gene expression related to breast cancer in blood.[29] By selecting top cis-QTLs within ±1,000 kb upstream and downstream of target genes with P-values < 5.0×10^{-8}, we demonstrated the superiority of the SMR method over conventional Mendelian randomization (MR) analysis under conditions of independence between exposure and outcome data. SNPs with allele frequency differences exceeding 0.2 were excluded, and the analysis focused on significant causal association signals among eQTLs. To enhance the reliability of these causal signals, P-values were adjusted to calculate false discovery rate (FDR) values, with FDR ≥ 0.05 serving as the threshold for exclusion. The heterogeneity of SMR analysis results across datasets was evaluated using the HEIDI test. In this study, SNPs with HEIDI P-values > 0.05 were selected to represent higher consistency between gene expression and disease association data.[30]

Obtain the Intersection Targets of XHP and Breast Cancer, and Conduct MR Analysis on Individual Targets

We identified the intersection targets by cross-referencing the drug targets of XHP with gene targets that met the SMR screening criteria. These intersection targets were considered as potential therapeutic targets of XHP in breast cancer. Subsequently, SMR analysis was performed on individual intersection targets (data sourced from eQTLGen) in relation to breast cancer (data from FinnGen). To validate the reliability of the associations between the intersection targets and breast cancer, two-sample MR analysis was conducted using the TwoSampleMR R package (version 0.5.8).[31] In this analysis, the intersection targets were used as exposures, with gene expression data obtained from eQTLGen, while the breast cancer outcome GWAS data were derived from the Breast Cancer Association Consortium (BCAC), which includes 122,977 cases and 105,974 controls of European ancestry, as well as 14,068 cases and 13,104 controls of East Asian ancestry.[32] To ensure robust causal inference, we selected instrumental variables (IVs) for each exposure (gene expression) at a stringent genome-wide significance threshold (P-values < 5.0×10^{-8}). This stringent selection minimizes weak instrument bias and increases the statistical power of the MR analysis. The use of large-scale GWAS summary statistics from the BCAC (comprising over 120,000 cases and 100,000 controls) provides high statistical power to detect modest but genuine causal effects of gene expression on breast cancer risk.

Chemicals and Reagents

XHP was purchased from Tong Ren Tang Technologies Co., Ltd. (Beijing, China; lot number: 22042652). The CCK-8 assay kit was obtained from Topscience Co., Ltd. (Shanghai, China). RPMI-1640 medium, fetal bovine serum (FBS), and penicillin-streptomycin (P/S) were purchased from Gibco (Thermo Fisher Scientific, Waltham, MA, USA). The BCA protein assay kit and RIPA lysis buffer were obtained from Solarbio (Beijing, China). The common protease inhibitor

cocktail and phosphatase inhibitor were from Proteintech (Rosemont, IL, USA). Clarity Western ECL substrate was from Bio-Rad (Hercules, CA, USA). Primary antibody against GAPDH (cat. no. ab9485) and goat anti-rabbit HRP-IgG (H&L) (cat. no. ab97040) were from Abcam (Cambridge, UK). Anti-GSTM1 rabbit monoclonal antibody (cat. no. HA721463) and anti-SLC22A5 rabbit monoclonal antibody (cat. no. ER64256) were from HUABIO (Hangzhou, China). The Servicebio® RT First Strand cDNA Synthesis Kit and 2×SYBR Green qPCR Master Mix (None ROX) were from Servicebio (Wuhan, China).

Cell and Culture Conditions

Human BC MDA-MB-231 and MCF-7 cells were acquired from the ATCC (Manassas, VA, USA). Both MDA-MB -231 cells and MCF-7 cells were grown in RPMI-1640, with both media containing 10% FBS and 1% P/S, at 37 °C in a 5% CO_2 incubator. Both cell lines used in the experiments were within 10 passages.

XHP-Containing Serum

Three-month-old female Sprague-Dawley rats were obtained from Shanghai SLAC Laboratory Animal Co., Ltd. (Shanghai, China), and they were randomized into three groups which contained 10 rats, respectively. The pills were pulverized and powdered before being intragastrically administered to the rats at 0 g/kg (normal saline served as control group), 1.5 g/kg (low-dose XHP cohort, referred as Low-XHP group in figures), and 3 g/kg (high-dose XHP group, referred as High-XHP group in figures) twice per day for three days. In addition, 2 h after the last administration, blood was collected, subjected to standing, centrifugation, inactivation, filtration, sterilization, and finally, the serum containing XHP and the control group serum with normal saline were both preserved in a refrigerator at −80 °C for further analysis. Subsequently, 10% XHP-containing serum was added to the medium for cell administration. The clinical dosage of XHP is 3g per time twice per day and we converted the dosage of human clinical administration into that of rats. XHP-containing serum was denoted to as XHP during in vitro experiments.

Ethical Approval

For Animal Studies

All animal protocols were carefully reviewed and received ethical approval from the Ethics Board of Zhejiang Provincial People's Hospital (Approval No. A20220068). All procedures were performed in accordance with the National Institutes of Health Guide for the Care and Use of Laboratory Animals (NIH Publications No. 8023, revised 1978) and were approved by the aforementioned Ethics Board.

Ethics Statement for Public Database Research

The network pharmacology analysis and Mendelian randomization study utilized only pre-existing, publicly available, and de-identified summary-level data from the TCMSP, SymMap, eQTLGen, FinnGen, and BCAC databases. No individual-level data were accessed, and no human participants were recruited specifically for this study. Therefore, in accordance with Article 32 of the "Measures for Ethical Review of Life Science and Medical Research Involving Human Subjects" (National Health Commission of China, effective February 18, 2023), which states that ethical review may be exempted for research using publicly available database information, this part of the work was exempt from requiring separate ethical approval from an institutional review board.

Small Interfering RNA (siRNA) Experiment

Chemically synthesized siRNA was introduced into cells via transfection with RNAiMAX Transfection Reagent. An siRNA directed against the luciferase gene (Sigma) served as the control.

Cell Viability Assessment

Cell viability was assessed using the CCK-8 assay under conditions of XHP exposure or following knockdown of intersection target genes. Cells (3×10^3 per well) were seeded in 96-well plates and cultured for 24 hours, after which the original medium was replaced. For drug treatment, cells were assigned to control, Low-XHP, or High-XHP groups and

incubated with corresponding serum-containing medium supplemented with XHP. In parallel experiments, transfected cells and untransfected controls (3×10^3 per well) were also cultured in 96-well plates. For drug treatment, cells were further incubated after the addition of XHP-containing serum for 24, 48, or 72 hours. For gene knockdown, cells were further incubated post-transfection for 24, 48, or 72 hours. At each time point, the medium was replaced with 100 μL of fresh medium containing 10% CCK-8 reagent, followed by incubation at 37 °C for 2 hours. Absorbance at 450 nm was measured using a microplate reader, and data were analyzed with GraphPad Prism 8.0 (La Jolla, CA, USA).

Wound Healing Assessment

Cell density was standardized to 5×10^5 cells per well, and cells were subsequently cultured in 6-well plates. When cell confluence reached approximately 80%–90%, a sterile 200 μL pipette tip was used to gently scrape the cell monolayer. Following this, cells were assigned to a control group, a low-concentration XHP group, or a high-concentration XHP group, and the corresponding XHP-containing serum culture medium was added. Sample images were captured immediately after wounding and medium replacement (0 hour) and after 24 hours of incubation using a 4× magnification microscope (EVOS M7000, Invitrogen). For the 231 cell line, an additional image was acquired at 12 hours. Scratch wound areas were quantified using Fiji software (ImageJ). Briefly, for each image, the scale was first set using the known scale bar. A rectangular region of interest (ROI) covering the entire scratch area and a consistent portion of the cell monolayer on both sides was defined. The image was converted to 8-bit, and a consistent threshold was applied to highlight the cell-free scratch area. The "Analyze Particles" function was then used to measure the scratch area in square micrometers (μm^2). The percentage of wound closure at each time point (T) was calculated as: [(Area at 0 hour – Area at T hour) / Area at 0 hour] × 100%.

Western Blotting

Total cellular proteins were extracted from each experimental group using RIPA lysis buffer, and protein concentrations were determined using the BCA assay. Equal amounts of protein (20 μg per sample) were loaded onto SDS-PAGE gels for electrophoretic separation. Following separation, proteins were transferred onto PVDF membranes (Millipore, Bedford, MA, USA). The membranes were blocked with 5% (w/v) skim milk to reduce nonspecific binding, then washed and incubated with primary antibodies diluted overnight at 4 °C. The antibodies and their dilutions were as follows: anti-GSTM1 rabbit monoclonal antibody (HUABIO, cat. no. HA721463) at 1:2000, anti-SLC22A5 rabbit monoclonal antibody (HUABIO, cat. no. ER64256) at 1:1500, and anti-GAPDH rabbit monoclonal antibody (Abcam, cat. no. ab9485) at 1:2500. Subsequently, the membranes were incubated with HRP-conjugated secondary antibodies diluted at 1:5000 (v/v) for 2 hours at room temperature. Immunoreactive signals were detected and visualized using Image Lab software (Bio-Rad).

RNA Extraction and Quantitative RT-PCR (qRT-PCR)

Total RNA was isolated from cells using the RNeasy Mini Kit and then reverse transcribed. qRT-PCR was performed on the ABI 7900HT Fast Real-Time PCR System. The relative transcriptional levels of the genes of interest were quantified using the $Ct(2^{-\Delta\Delta}Ct)$ method. The primers are listed in Table 1.

Statistical Analysis

Data are presented as mean ± standard deviation (SD) from three independent experiments (n=3) and analyzed using GraphPad Prism version 7.0 software (La Jolla, CA, USA). Differences between groups were evaluated using one-way analysis of variance (ANOVA) followed by Tukey's tests. $p < 0.05$ was considered statistically significant.

Results

Identification of Active Targets of XHP

The four primary ingredients of XHP—bezoar, musk, myrrh, and frankincense—were systematically screened using the TCMSP and Symmap databases according to predefined selection criteria. The corresponding active compounds and their

Table 1 PCR Primer Sequences

Gene	Forward Primer (5'→3')	Reverse Primer (5'→3')
SLC22A5	GGACCAGAAACTTAACAACGACG	CAGGCTGTGTGAATGGACCT
GSTM1	ACTTGATTGATGGGGCTCAC	TCTCCAAAATGTCCACACGA

associated target proteins were collected. After removing duplicate targets, a total of 383 potential XHP-target interactions were identified (Supplementary Box 1).

GO&KEGG Analyses

GO analysis showed XHP targets were enriched in Biological Processes related to responses to peptides, xenobiotics, bacterial molecules, lipopolysaccharide, and hypoxia. At the Cellular Component level, targets were mainly in plasma membrane structures, including the external side, vesicle lumen, membrane microdomain, and membrane raft. For Molecular Function, targets were linked to transcription-regulating activities such as DNA-binding transcription factor binding, RNA polymerase II-specific transcription factor binding, ligand-activated transcription factor activity, nuclear receptor activity, and transcription coregulator binding.

KEGG analysis identified key pathways: "Lipid and atherosclerosis," "Chemical carcinogenesis - receptor activation," "Fluid shear stress and atherosclerosis," "AGE-RAGE signaling pathway in diabetic complications," and "Prostate cancer" (Figure 2; full results in Supplementary Material 1).

Identification of Breast Cancer-Related Genes via Mendelian Randomization

By integrating the eQTLGen blood expression quantitative trait loci (eQTL) data with FinnGene breast cancer GWAS data, we conducted SMR analysis to explore the potential causal relationship between gene expression levels and breast cancer risk. After multiple testing correction (FDR < 0.05) and heterogeneity test (HEIDI test $p > 0.05$), a total of 33 significant genes were identified. Among them, the RCCD1 gene showed the strongest association signal (b_SMR = −0.103, p_SMR = 9.61×10^{-9}, FDR = 2.36×10^{-5}), suggesting that an increase in its expression level may reduce the risk of breast cancer. Other key genes include: NEK10 (b_SMR = −1.567, p_SMR = 2.14×10^{-7}), FGFR2 (a known breast cancer susceptibility gene, b_SMR =

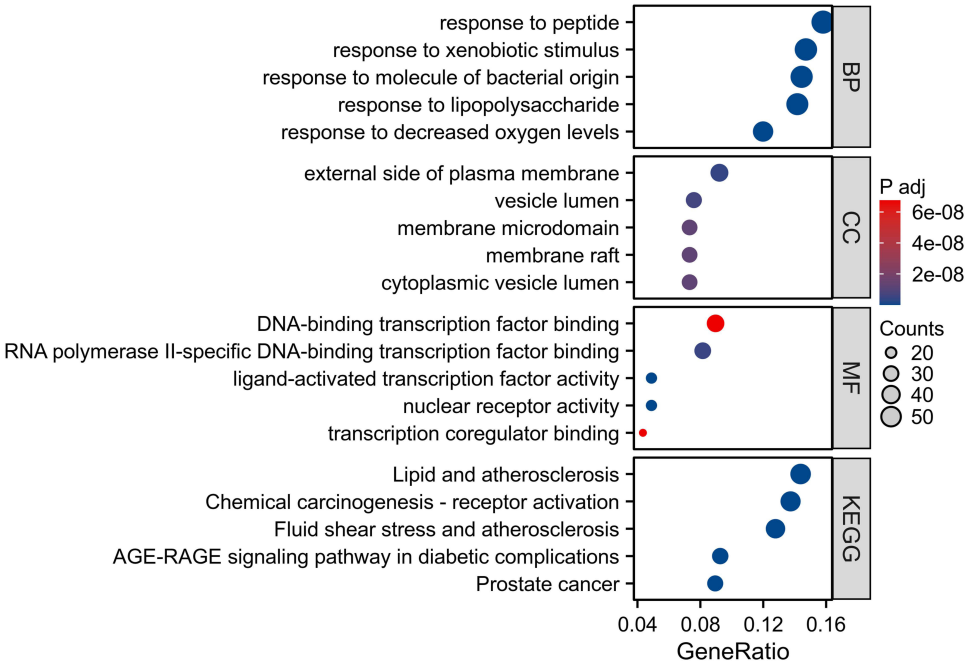

Figure 2 GO&KEGG Plot.

https://doi.org/10.2147/BCTT.S572244

0.099, p_SMR = 6.75×10^{-5}), SLC22A5 (b_SMR = −0.069, p_SMR = 7.80×10^{-6}), and GSTM1 (b_SMR = −0.092, p_SMR = 1.45×10^{-5}). The HEIDI test results of all significant genes (p_HEIDI > 0.05) support the single causal variant model and rule out linkage disequilibrium confounding (Table 2). These findings suggest that the expression levels of specific genes in the blood may affect the risk of breast cancer through regulatory pathways. All results are presented in Supplementary Material 2.

Venn Diagram Analysis

By integrating the pharmacological action targets of XHP with the 33 significant genes (FDR < 0.05) identified through SMR analysis of breast cancer, we discovered two key intersecting genes: GSTM1, SLC22A5. A Venn diagram was generated to illustrate these overlapping targets, suggesting they may be crucial targets for XHP in treating breast cancer (Figure 3).

Perform SMR Analysis on the Intersecting Targets

Using SMR analysis, we systematically examined the causal relationship between the expression levels of key genes GSTM1 and SLC22A5 and breast cancer risk. The Effect Plot for GSTM1 (Figure 4A) revealed a statistically significant

Table 2 Results of SMR

Gene	probeID	GWAS effect (p-value)	eQTL effect (p-value)	Pvalue_SMR	Pvalue_HEIDI	fdr
RCCD1	ENSG00000166965	−0.0817 (8.60e-09)	0.7968 (0.00e+00)	9.61319E-09	0.99496760	2.35986E-05
NEK10	ENSGO0000163491	0.1018 (8.47e-20)	−0.0650 (2.78e-10)	2.13595E-07	0.22106090	0.00029961
ATG10	ENSGO0000152348	−0.0636 (2.28e-07)	0.5060 (0.00e+00)	2.56556E-07	0.14532620	0.000327155
KCNN4	ENSG00000104783	0.0529 (5.01e-07)	0.6318 (0.00e+00)	5.25139E-07	0.37285630	0.000613843
LYPD5	ENSG00000159871	0.0491 (9.88e-07)	−0.1202 (5.69e-52)	3.19784E-06	0.05862502	0.002990411
PDS5A	ENSG00000121892	0.0496 (2.79e-06)	0.1786 (3.34e-101)	4.72217E-06	0.54727570	0.004139862
SLC22A5	ENSG00000197375	0.0472 (7.62e-06)	−0.6807 (0.00e+00)	7.79603E-06	0.10502920	0.00575552
GSTM1	ENSG00000134184	−0.0529 (1.38e-05)	0.5758 (0.00e+00)	1.45247E-05	0.11483040	0.00848906
RRP1B	ENSG00000160208	0.0461 (1.82e-05)	0.1738 (6.25e-102)	2.64075E-05	0.40419440	0.01419555
HSF2BP	ENSGO0000160207	0.0503 (1.55e-06)	0.0715 (7.70e-18)	2.73244E-05	0.24380060	0.01419555
PABPC4	ENSG00000090621	0.0574 (2.12e-05)	−0.2422 (1.27e-107)	2.9813E-05	0.31133380	0.01493527
SNX32	ENSG00000172803	0.0565 (5.24e-05)	0.3692 (5.68e-287)	5.82933E-05	0.12559390	0.02265143
IRF1	ENSG00000125347	0.0475 (1.07e-05)	0.0802 (1.62e-22)	5.98424E-05	0.05991738	0.02265143
ZDHHC18	ENSG00000204160	0.0556 (5.65e-05)	0.4279 (0.00e+00)	6.13641E-05	0.91099190	0.02265143
FGFR2	ENSG00000066468	−0.0402 (6.44e-05)	−0.4052 (0.00e+00)	6.75174E-05	0.05626984	0.02428377
PNKD	ENSG00000127838	−0.0437 (8.15e-05)	−0.5315 (0.00e+00)	8.35993E-05	0.17591000	0.02649133
MCM3AP-AS1	ENSG00000215424	0.0506 (6.88e-05)	−0.3012 (2.05e-135)	8.49868E-05	0.12440550	0.02649133
MAFF	ENSG00000185022	−0.0412 (5.83e-05)	0.1323 (3.28e-61)	9.40936E-05	0.18098110	0.02792131
PRC1-AS1	ENSG00000258725	−0.0497 (4.94e-05)	−0.3483 (6.97e-44)	9.79877E-05	0.07482879	0.02792131
SLC35E3	ENSG00000175782	−0.0543 (9.71e-05)	−0.4334 (0.00e+00)	0.000102829	0.42213660	0.02792131
YBEY	ENSG00000182362	0.0457 (1.01e-04)	0.7754 (0.00e+00)	0.000103172	0.32197610	0.02792131
AKAP9	ENSGO0000127914	0.0442 (1.80e-05)	−0.0748 (6.20e-20)	0.000103508	0.06776937	0.02792131
GPBAR1	ENSG00000179921	−0.0415 (1.47e-04)	0.2415 (2.09e-196)	0.000166315	0.93094670	0.03481931
UBXN6	ENSG00000167671	−0.0385 (1.39e-04)	0.1791 (1.77e-112)	0.000172579	0.05746993	0.03559943
CCNA2	ENSG00000145386	0.0397 (9.24e-05)	−0.0963 (1.17e-31)	0.000208515	0.17589850	0.04020209
LINC01814	ENSG00000236008	−0.0405 (1.84e-04)	−0.5723 (3.12e-176)	0.000209222	0.05711906	0.04020209
ARRDC3	ENSG00000113369	−0.0587 (5.98e-05)	−0.1048 (2.14e-21)	0.000218117	0.71817000	0.04134499
LAMTOR5	ENSG00000134248	0.0372 (2.04e-04)	0.2409 (7.01e-167)	0.000233119	0.23342430	0.04302584
CENPW	ENSG00000203760	0.0395 (8.38e-05)	−0.0955 (2.15e-24)	0.000243079	0.29197030	0.04423798
GIMAP8	ENSG00000171115	−0.0375 (2.51e-04)	−0.3098 (0.00e+00)	0.000266521	0.79796460	0.04680055
JAZF1	ENSGO0000153814	0.0369 (2.63e-04)	0.4639 (0.00e+00)	0.000270253	0.29360390	0.04680055
FCHO2	ENSGO0000157107	−0.0370 (2.89e-04)	0.5600 (0.00e+00)	0.000293081	0.25533340	0.0494762
SUB1	ENSGO0000113387	−0.0401 (7.61e-05)	0.0724 (3.59e-19)	0.000296286	0.09092881	0.0494762

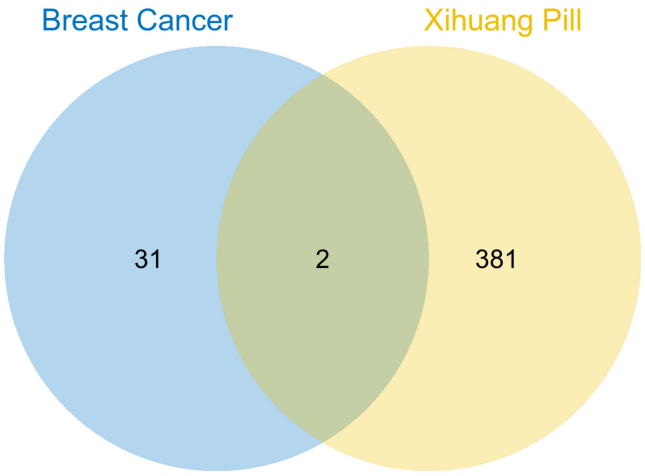

Figure 3 Venn diagram of Xihuang Pill and Breast Cancer.

inverse association between its expression level and breast cancer risk (β_SMR = −0.092, p_SMR = 1.45×10^{-5}). The top cis-eQTL at rs11101992 (red triangle) exhibited the strongest effect (β_eQTL = 0.576, β_GWAS = −0.053), indicating that a one-unit increase in GSTM1 expression was associated with a 5.3% reduction in breast cancer risk. Locus Plot analysis (Figure 4B) further demonstrated that, within a 500 kb region flanking the GSTM1 gene, the rs11101992 locus passed the HEIDI test (p_HEIDI = 0.11), supporting a single causal variant model. No evidence of pleiotropic confounding was observed in this genomic region.

The SLC22A5 gene also exhibited a negative association (β_SMR = - 0.069, p_SMR = 7.80×10^{-6}). In its Effect Plot (Figure 4C), the top cis - eQTL rs11242109 (β_eQTL = - 0.681, β_GWAS = 0.047) suggested that a reduction in SLC22A5 expression was correlated with an elevated risk of breast cancer. The Locus Plot (Figure 4D) indicated that the genetic signal within this gene region passed the HEIDI test (p_HEIDI = 0.11), with no indication of pleiotropy. It is noteworthy that there are multiple breast - cancer - related genes in this region (such as IRF1), yet SLC22A5 demonstrated the most robust independent signal.

Perform a Two-Sample MR Analysis on the Intersecting Targets

To evaluate the causal association between GSTM1 gene expression and breast cancer risk, we performed a two-sample MR analysis. A total of 10 independent genetic variants significantly linked to GSTM1 expression were selected as instrumental variables, all of which passed stringent quality control criteria ($p < 5\times10^{-8}$). The primary analysis was conducted using the inverse-variance weighted (IVW) method, which demonstrated that each unit increase in GSTM1 expression was associated with a 4.4% reduction in breast cancer risk (OR = 0.9568, 95% CI: 0.9205–0.9947, p = 0.0257) (Table 3). This protective effect was consistently supported by complementary MR approaches, including the weighted median method (OR = 0.9391, p = 0.0007), weighted mode method (OR = 0.9407, p = 0.0061), and MR-Egger method (OR = 0.8977, p = 0.0270).

The pleiotropy test showed that the MR-Egger intercept was not statistically significant (intercept = 0.0542, p = 0.1126), indicating that the results were not affected by directional pleiotropy (Table 3). The heterogeneity test suggested that IVW had mild heterogeneity (Cochran's Q = 15.05, p = 0.0897), but MR-Egger did not detect heterogeneity (Q = 10.77, p = 0.2150). The MR effect forest plot was shown in Figure 5A. The leave-one-out sensitivity analysis confirmed that no single SNP dominated the results (Figure 5B), and the scatter plot showed that all instrumental variables had a negative effect trend (Figure 5C). The funnel plot was symmetrically distributed (Figure 5D), further supporting the robustness of the results.

To evaluate the causal association between SLC22A5 gene expression and breast cancer risk, we performed a two-sample MR analysis using five independent genetic variants as instrumental variables significantly associated with SLC22A5 expression (all meeting genome-wide significance, $p < 5\times10^{-8}$, and passing rigorous quality control). The

https://doi.org/10.2147/BCTT.S572244

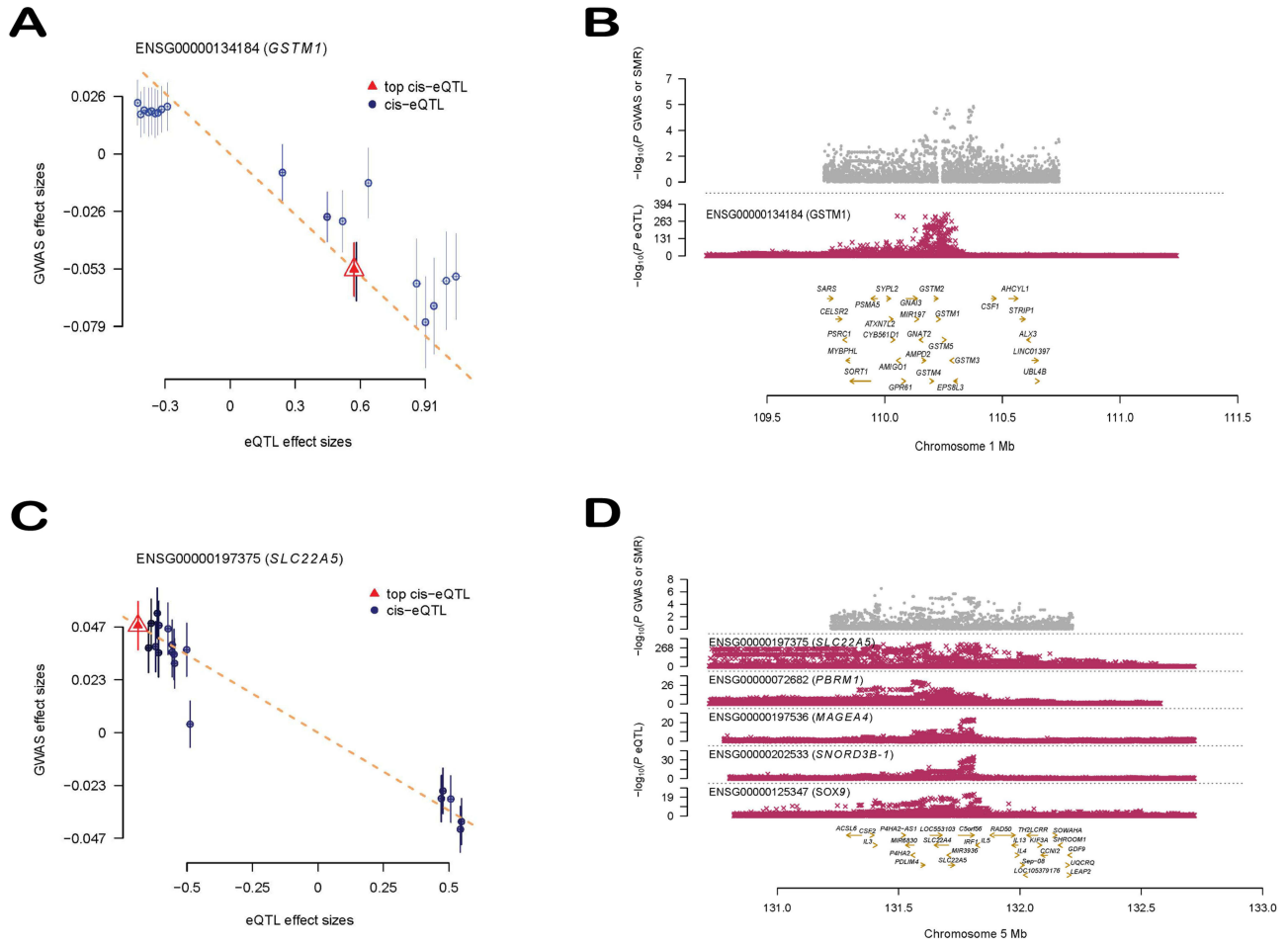

Figure 4 Single-gene SMR analysis. (**A**) GSTM1 Effect Plot; (**B**) GSTM1 Locus Plot; (**C**) SLC22A5 Effect Plot; (**D**) SLC22A5 Locus Plot.

primary analysis, based on the IVW method, revealed that each unit increase in genetically predicted SLC22A5 expression was associated with a 3.0% reduction in breast cancer risk (OR = 0.9700, 95% CI: 0.9426–0.9983, p = 0.0378; Table 3). Sensitivity analyses yielded consistent directional effects: the weighted median method showed a similar trend (OR = 0.9713, p = 0.0997), albeit marginally significant, while the weighted mode method indicated a non-significant protective effect (OR = 0.9723, p = 0.1563). The MR-Egger regression, which accounts for potential pleiotropy, produced an OR of 1.0045 (p = 0.9236), suggesting no significant causal effect under this model and

Table 3 Results of Two-Sample MR

Gene	Method	OR (95%CI)	P-value	Q	Q_pval	Intercept	Pleiotropy_pval
GSTM1	Inverse variance weighted 0	0.96 (0.92,0.99)0	0.026	5.05	0.090		
GSTM1	MR Egger	0.90 (0.83,0.97)0.0	27 10.	770.2	15 0	0.054	0.113
GSTM1	Weighted median	0.94 (0.91,0.97)	0.00073				
GSTM1	Simple mode	0.96 (0.89,1.03)	0.244				
GSTM1	Weighted mode	0.94 (0.91,0.97)	0.006				
SLC22A5	Inverse variance weighted	0.97 (0.94,1.00)	0.038	2.63	0.621		
SLC22A5	MR Egger	1.00 (0.92,1.09)	0.924	1.89	0.596	−0.015	0.451
SLC22A5	Weighted median	0.97 (0.94,1.01)	0.100				
SLC22A5	Simple mode	0.94 (0.90,0.99)	0.073				
SLC22A5	Weighted mode	0.97 (0.94,1.00)	0.156				

https://doi.org/10.2147/BCTT.S572244

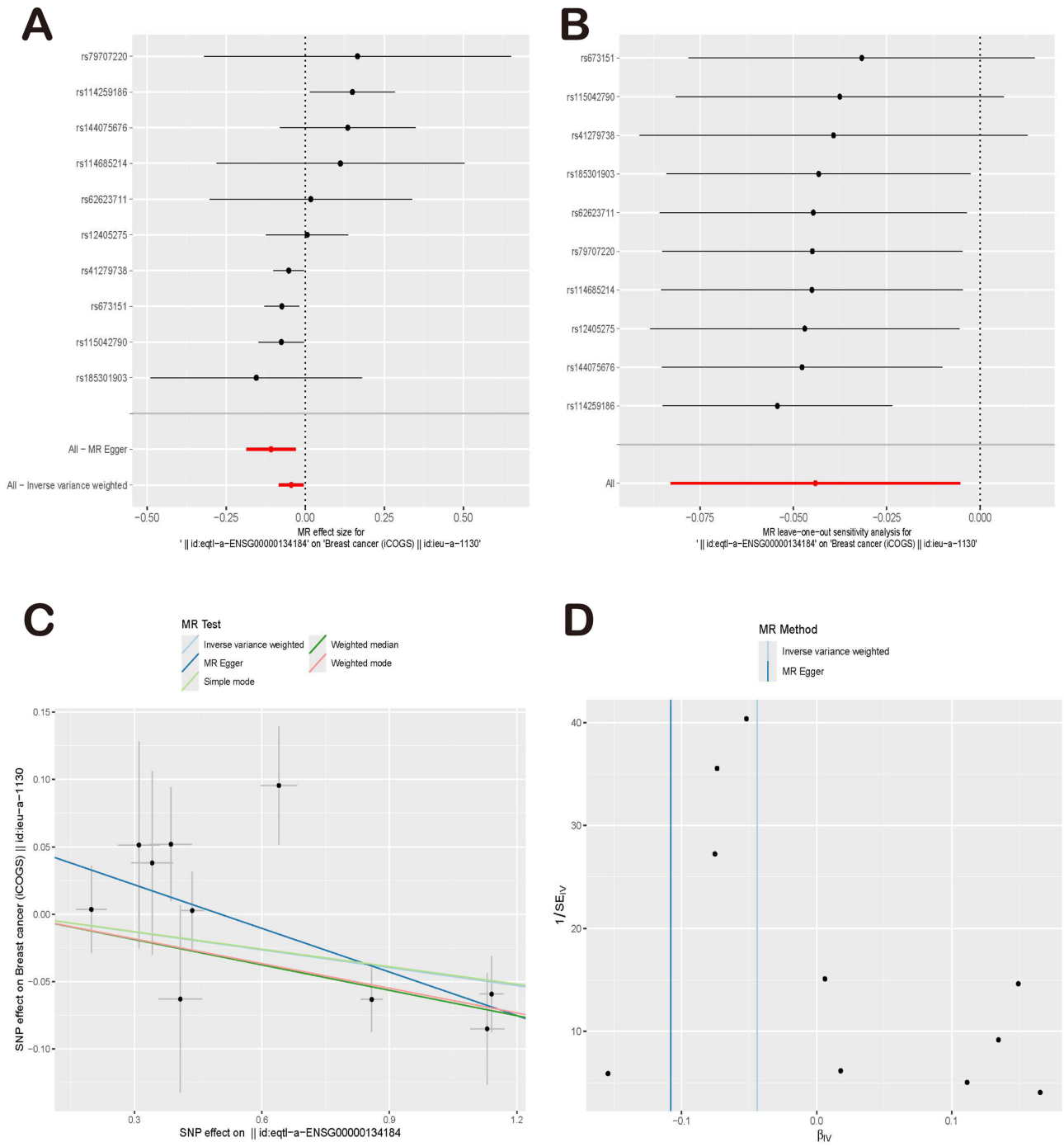

Figure 5 MR of GSTM1. (**A**) forest plot; (**B**) leave-one-out analysis plot; (**C**) scatter plot; (**D**) funnel plot.

indicating that horizontal pleiotropy may not be driving the observed association. Collectively, these results support a robust and modest inverse causal relationship between SLC22A5 expression and breast cancer risk.

The MR-Egger intercept test for pleiotropy revealed no evidence of directional pleiotropy (intercept = −0.0152, p = 0.4507), suggesting that the observed causal estimate is unlikely to be biased by systematic pleiotropic effects. Heterogeneity assessments indicated no significant heterogeneity in either the IVW or MR-Egger models (IVW Cochran's Q = 2.63, p = 0.6208; MR-Egger Q = 1.89, p = 0.5964), further supporting the homogeneity of the instrumental variable effects (Table 3). The MR effect forest plot was shown in Figure 6A. Leave-one-out sensitivity analysis confirmed the robustness of the causal estimate, as the direction of the effect remained consistent across all

https://doi.org/10.2147/BCTT.S572244

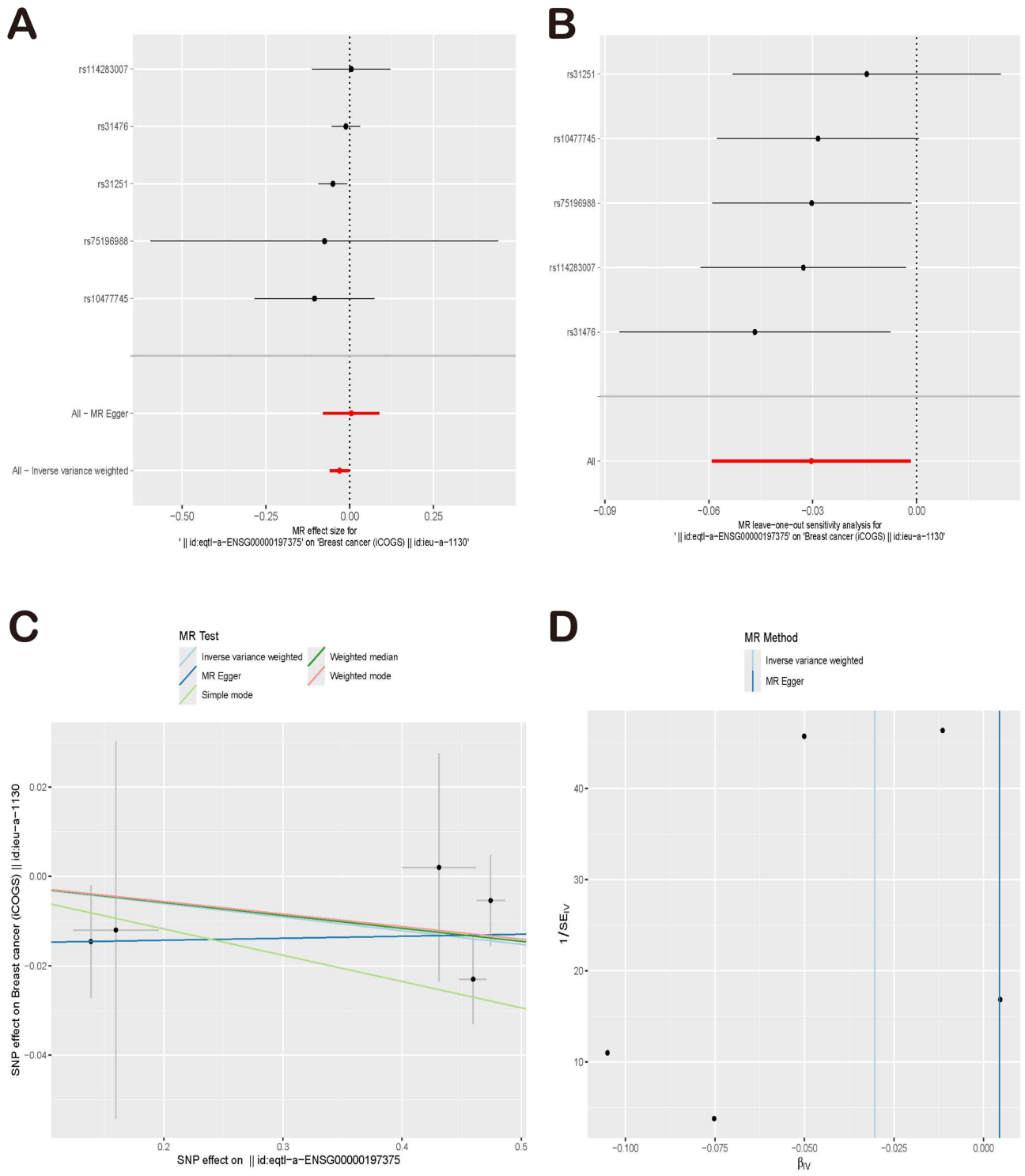

Figure 6 MR of SLC22A5. (**A**) forest plot; (**B**) leave-one-out analysis plot; (**C**) scatter plot; (**D**) funnel plot.

iterations when each SNP was sequentially excluded (Figure 6B). Notably, removal of the dominant instrument rs31251 (β_exposure = −0.460) resulted in a stronger protective association (OR = 0.940), suggesting this variant may have a moderating influence on the overall effect. Visual inspection of the scatter plot revealed a predominant negative trend among the genetic instruments (Figure 6C), and the funnel plot exhibited symmetrical distribution (Figure 6D), both of which support the reliability and validity of the MR findings.

Silencing SLC22A5 and GSTM1 Promotes the Proliferation and Migration of Breast Cancer Cells

To verify the reliability of the above Mendelian randomization results, we conducted cell experiments. We selected two breast cancer cell lines, MCF-7 and MDA-MB-231, and used siRNA to knock down the expression of GSTM1 and SLC22A5 in each cell line respectively. WB and qPCR experiments demonstrated the knockdown effect of siRNA on SLC22A5/GSTM1 (Figure 7A and B). To evaluate migration capacity, scratch assays demonstrated that silencing either GSTM1 or SLC22A5 significantly increased the migratory ability of both breast cancer cell lines. As shown in Figure 7C, cells in the siNC groups displayed loosely arranged edges at the wound site, whereas the knockdown groups exhibited a dense, front-edge migration band, indicative of accelerated collective cell movement. We assessed the proliferation dynamics of MCF-7 and MDA-MB-231 cells following specific siRNA-mediated silencing of target genes using the CCK-8 assay. In MCF-7 and 231 cells, the negative control group (siNC) exhibited a typical time-dependent increase in cell viability, peaking on day 4. In contrast, in MCF-7 cells, knockdown of GSTM1 (si1 and si2) increased cell viability by 71.05 (95% CI: 38.23–103.9) and 132.1 (95% CI: 99.26–164.9), respectively; knockdown of SLC22A5 (si1 and si2) increased cell viability by 138.9 (95% CI: 106.1–171.7) and 182.2 (95% CI: 149.4–215.0), respectively, with all comparisons being statistically significant ($p < 0.0001$). Similarly, in 231 cells, knockdown of GSTM1 (si1 and si2) increased cell viability by 107 (95% CI: 79.18–134.8) and 90.63 (95% CI: 62.84–118.4), respectively; knockdown of SLC22A5 (si1 and si2) increased cell viability by 255.5 (95% CI: 227.7–283.3) and 200.3 (95% CI: 172.5–228.1), respectively, with all comparisons being statistically significant ($p < 0.0001$). (Figure 7D). The above data collectively confirm that the expressions of GSTM1 and SLC22A5 are both negatively correlated with the proliferation ability of breast cancer cells, which is consistent with the results of Mendelian randomization experiments.

The Regulatory Effect of XHP on Target Genes

To investigate the regulatory effects of XHP on target genes, we performed Western blotting (WB) and quantitative real-time PCR (qRT-PCR) assays. Western blot analysis showed that in two breast cancer cell lines treated with drug-containing serum at varying concentrations of XHP, the protein levels of SLC22A5 and GSTM1 were upregulated in a dose-dependent manner, with stable expression of GAPDH (36 kDa) serving as the loading control (Figure 8A). Consistently, qRT-PCR results demonstrated that mRNA expression levels of both GSTM1 and SLC22A5 were significantly increased in a concentration-dependent fashion following treatment (Figure 8B). These findings indicate that XHP specifically enhance the expression of these two target genes at both the protein and transcriptional levels in breast cancer cells, aligning with the protective direction predicted by prior Mendelian randomization analysis.

XHP Suppress the Proliferation and Migration of Breast Cancer Cells

Finally, to validate the inhibitory effects of XHP on breast cancer cells, we performed CCK-8 and scratch assays. CCK-8 analysis revealed that in both cell lines, cancer cell proliferation was significantly suppressed following treatment with either low or high concentrations of XHP-containing serum compared to the control group. On day 4, the mean differences in cell viability between the NC and XHP L groups and between the NC and XHP H groups were 82.38 (95% CI: 58.97 to 105.8; $p < 0.0001$) and 80.15 (95% CI: 56.74 to 103.6; $p < 0.0001$) in 231 cells, respectively. In MCF-7 cells, the corresponding values were 81.77 (95% CI: 49.93 to 113.6; $p < 0.0001$) and 71.74 (95% CI: 39.90 to 103.6; $p < 0.0001$), respectively. However, this inhibitory effect did not exhibit a clear dose-dependent relationship (Figure 9A). Scratch assay results showed that, at 24 hours post-wounding, both treatment groups displayed significantly reduced wound healing rates relative to the normal control group, demonstrating that XHP-containing serum markedly suppresses the migratory capacity of both breast cancer cell lines (Figure 9B).

Discussion

Traditional Chinese medicine has been employed in the treatment of cancer-like conditions in China for over a thousand years, with extensive documentation found in ancient Chinese medical texts.[33] XHP is a classic clinical formula in traditional Chinese medicine, known for its functions of reinforcing the body's vital foundation, tonifying qi and blood, promoting blood circulation to resolve stasis, and softening and dispersing hard masses. They have long been used in the

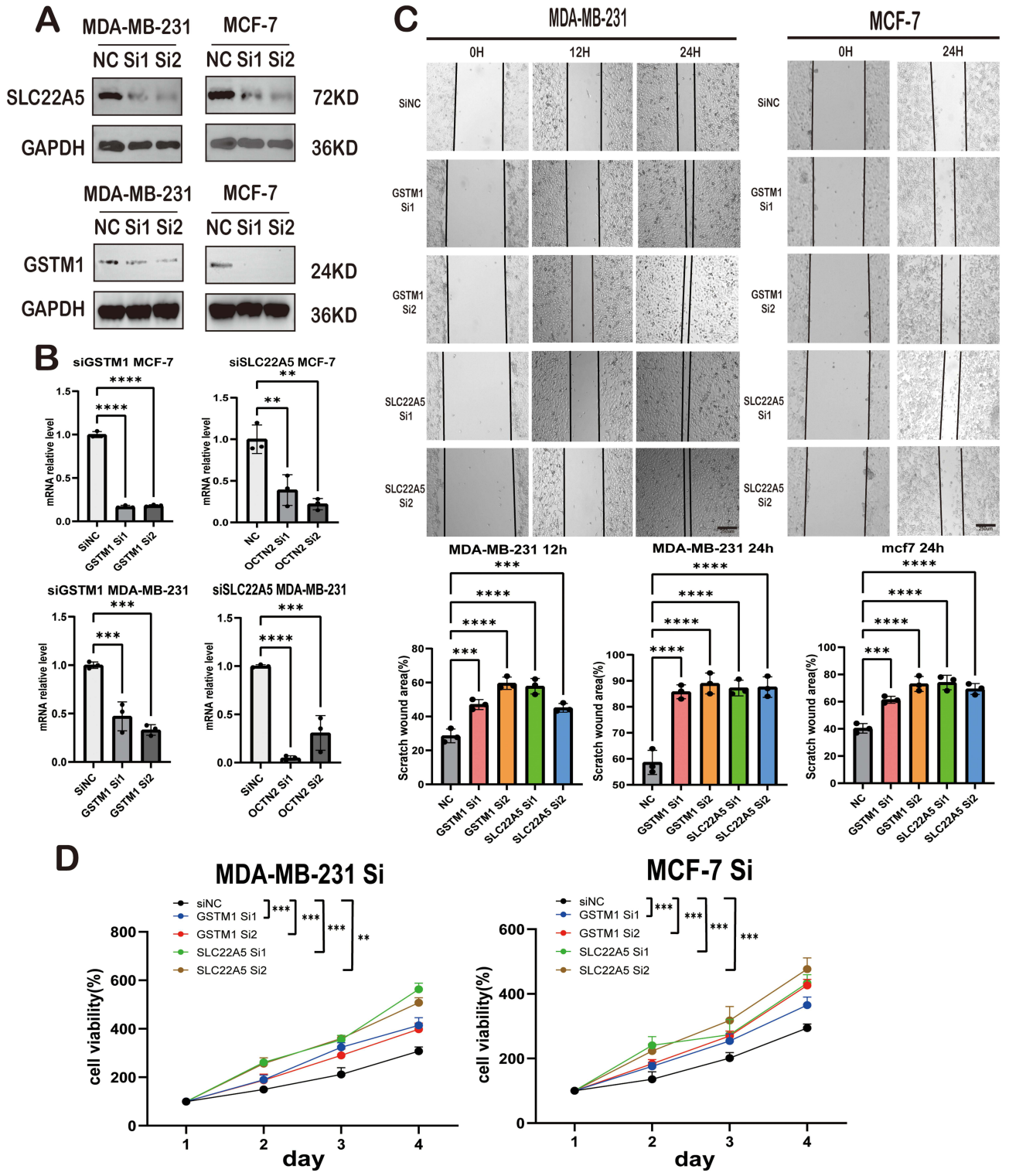

Figure 7 (**A**) WB: knockdown effect of siRNA; (**B**) PCR: knockdown effect of siRNA; (**C**) wound healing assays of cells treated with SiRNA; (**D**) proliferation of cells treated with SiRNA. Data provided as mean ± SD. All experiments were repeated three times. "**" stands for $P<0.01$, "***" stands for $P<0.001$ and "****" stands for $P<0.0001$.

treatment of cancer.[10] In recent years, with increasingly in-depth research on XHP, their therapeutic effects have been demonstrated in various cancers, including breast cancer, lung cancer, glioblastoma, liver cancer, and prostate cancer. Notably, XHP exhibits substantial potential as a therapeutic agent in breast cancer.[9,34–36] Existing studies have

https://doi.org/10.2147/BCTT.S572244

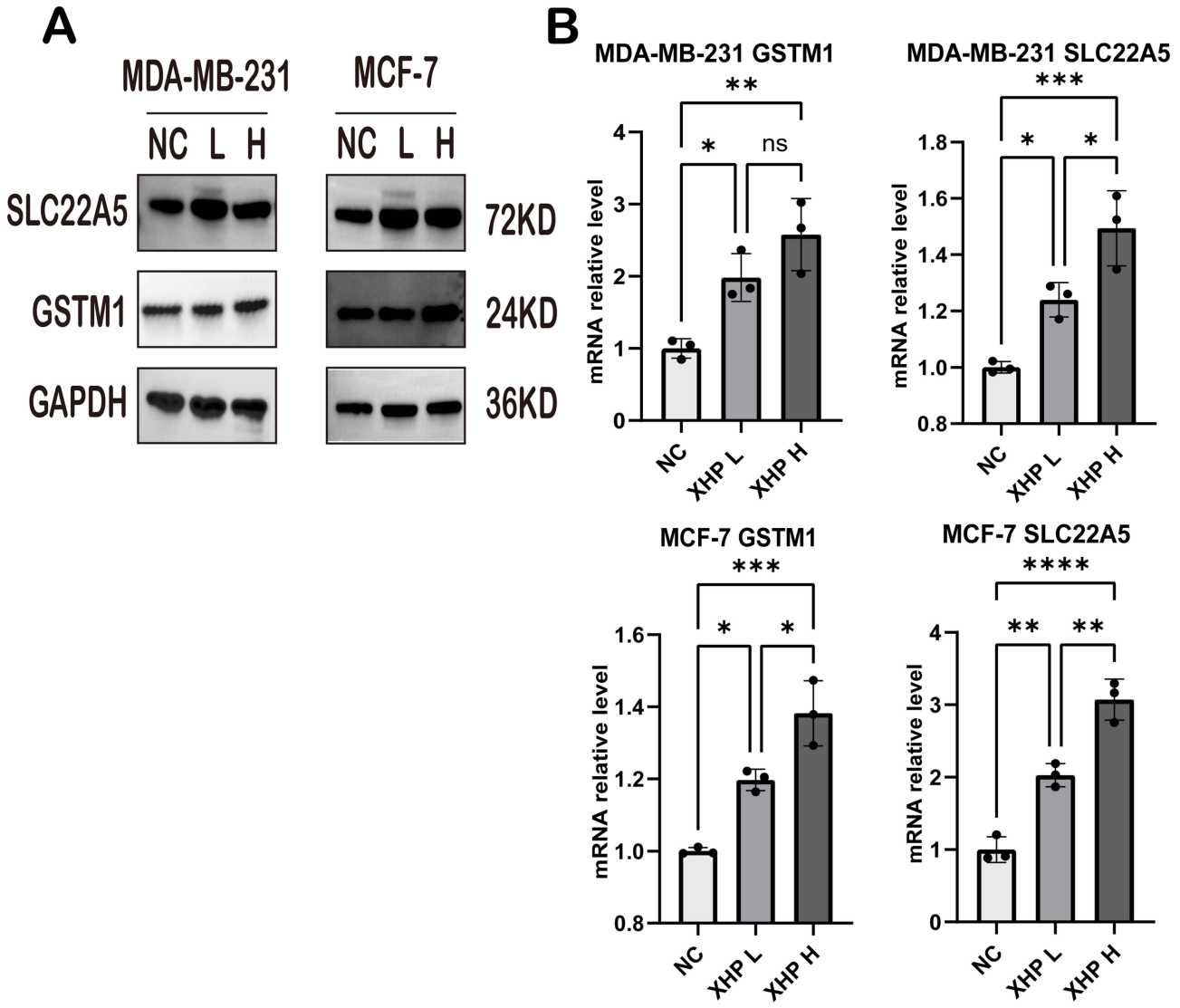

Figure 8 (**A**) the protein levels of SLC22A5 and GSTM1 after being treated with XHP; (**B**) mRNA expression levels of SLC22A5 and GSTM1 after being treated with XHP. Data provided as mean ± SD. All experiments were repeated three times. "ns" stands for nonsignificant, "*" stands for $P<0.05$, "**" stands for $P<0.01$, "***" stands for $P<0.001$ and "****" stands for $P<0.0001$.

demonstrated that XHP suppress the epithelial-mesenchymal transition (EMT) via the TGF-β signaling pathway, thereby inhibiting tumor metastasis. They also promote breast cancer cell apoptosis by activating the mitochondrial apoptotic pathway through ERK signaling. Furthermore, XHP can enhance the therapeutic efficacy of the chemotherapeutic agent doxorubicin (Dox).[37,38] Notably, Yebei Qiu et al reported that XHP inhibit OTUB1-mediated deubiquitination of SLC7A11, leading to SLC7A11 protein degradation, subsequent suppression of the system Xc^-/GPX4 axis, and induction of ferroptosis in triple-negative breast cancer (TNBC) cells, contributing to their anti-tumor activity.[39] However, as a traditional Chinese medicine formula, XHP are characterized by multiple bioactive components and multi-target actions, and their underlying anti-tumor mechanisms require further systematic investigation.

Over the past decade, the widespread application of network pharmacology and Mendelian randomization in identifying drug targets and elucidating mechanisms of drug action has led to the discovery of numerous novel therapeutic targets for diseases, as well as the recognition of repurposing potential for many existing drugs. In this study, we systematically identified the target genes of the four principal components of XHP using network

https://doi.org/10.2147/BCTT.S572244

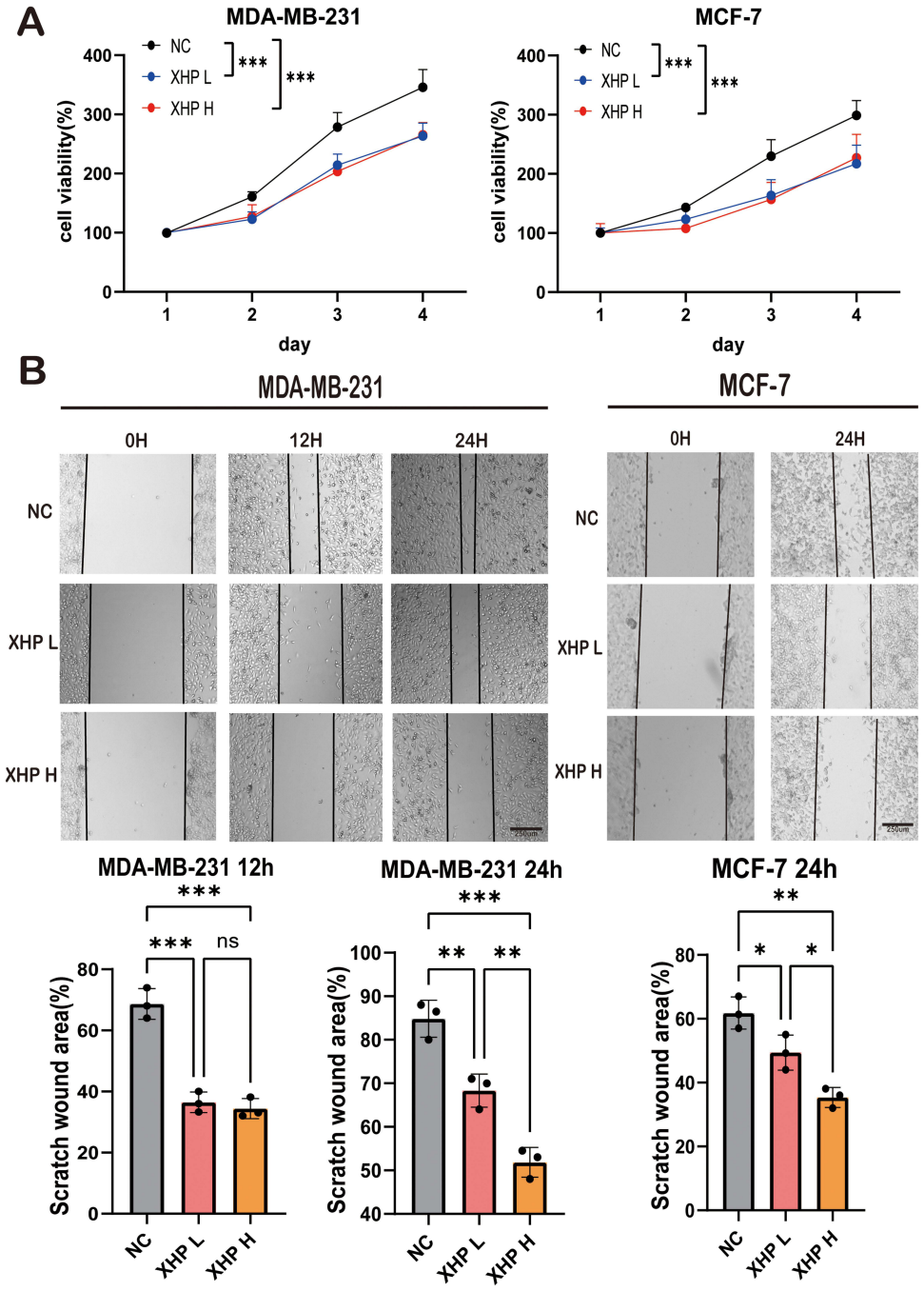

Figure 9 (**A**) proliferation of cells treated by XHP; (**B**) wound healing assays of cells treated with XHP. Data provided as mean ± SD. All experiments were repeated three times. "*" stands for $P<0.05$, "**" stands for $P<0.01$ and "***" stands for $P<0.001$, "ns" stands for nonsignificant.

pharmacology, and by integrating Mendelian randomization analysis, successfully pinpointed two genes strongly associated with breast cancer: GSTM1 and SLC22A5.

GSTM1 is one of the most prevalent isoforms of glutathione S-transferase (GST) and plays a critical role in cellular detoxification. It catalyzes the conjugation of glutathione with electrophilic substrates, including reactive oxygen species (ROS) and reactive aldehydes (RAs), thereby protecting cells against oxidative damage induced by lipid peroxidation and other oxidative stressors.[40] In oncology, GSTM1 has also been implicated in various malignancies, including breast cancer. Research by Sharda P Singh et al revealed that GSTM1 expression is significantly downregulated in the MammaPrint High 2 (highest-risk group) and BluePrint Basal (basal-like subtype) subtypes of breast cancer, making it

 https://doi.org/10.2147/BCTT.S572244

one of the most differentially expressed genes. Low GSTM1 expression is associated with poorer overall survival (OS) and exhibits a negative correlation with tumor invasiveness. This study also found that the glutathione metabolic process where GSTM1 is located was significantly enriched in the High 2 and Basal groups, suggesting that this pathway plays a significant role in the progression of breast cancer. Therefore, GSTM1 was identified as a protective gene in this study, with its low expression closely related to high risk of breast cancer, Basal subtype, poor prognosis, and abnormal glutathione metabolic process. It may serve as a potential prognostic biomarker, especially valuable in identifying high-risk patients who may be less sensitive to chemotherapy.[41] Meanwhile, numerous studies have found that consuming cruciferous vegetables can reduce the risk of breast cancer,[42,43] and sulforaphane, a bioactive compound in cruciferous vegetables, can precisely induce the expression of antioxidant enzymes including GSTM1 by activating the Nrf2 pathway.[40] Yingyan Yu and others discovered through pan-genome analysis that GSTM1 is a frequently deleted gene in the Chinese gastric cancer population. Its deletion may be associated with abnormal chemical carcinogen metabolic pathways, thereby increasing the risk of gastric cancer.[44] Similar findings have been made for GSTM1 in bladder cancer. A study confirmed through GWAS meta-analysis that GSTM1 is a susceptibility gene for bladder cancer. Individuals with the null genotype of GSTM1 have an increased susceptibility to bladder cancer, especially among smokers. Moreover, higher plasma GSTM1 levels are significantly associated with a reduced risk of bladder cancer, suggesting that it may be related to the metabolic clearance of carcinogens such as polycyclic aromatic hydrocarbons in tobacco smoke by GSTM1.[45] The above-mentioned studies on GSTM1 in breast cancer all suggest that it has a protective effect on tumors. The findings of our study also confirm that the downregulated expression of GSTM1 enhances the proliferation and migration capabilities of breast cancer 231 and MCF7 cells.

SLC22A5, also known as OCTN2 (Organic Cation/Carnitine Transporter 2), is a high-affinity transporter for carnitine and plays a central role in cellular carnitine uptake. It also exhibits transport activity toward choline. This transporter is highly expressed in the kidneys, intestines, skeletal muscle, and placenta,[46] and its genetic mutations are causally linked to systemic carnitine deficiency.[47] Notably, due to its high-affinity recognition and transport of carnitine, SLC22A5 has been implicated in the cellular uptake of several chemotherapeutic agents, such as oxaliplatin and imatinib.[48,49] Leveraging this property, Kou Longfa et al developed carnitine-modified nanoparticles to enhance drug delivery across the blood-brain barrier and achieve targeted delivery to glioma cells.[50] Previous studies have indicated that SLC22A5 is upregulated in breast cancer, particularly in estrogen receptor-positive (ER+) subtypes. siRNA-mediated knockdown of SLC22A5 has been shown to suppress breast cancer cell proliferation. This inhibitory effect is hypothesized to result from impaired carnitine transport, leading to dysregulated lipid metabolism and reduced cellular energy production, ultimately hindering tumor cell growth.[51] Ji-Hyun Lee et al identified SLC22A5 as a driver gene harboring recurrent mutations in metastatic breast cancer. The mutation may promote cancer cell migration and distant metastasis through modulation of the epithelial-mesenchymal transition (EMT) pathway, particularly via upregulation of ZEB1. This genetic alteration represents a potential biomarker for early identification of breast cancer patients at high risk of metastasis.[52] The results of our study suggest that the reduced expression of SLC22A5 inhibits the proliferation and migration of breast cancer 231 and MCF7 cells, which diverges from previous reports. This apparent paradox could be resolved by considering tumor subtype specificity and metabolic microenvironment. For instance, in aggressive subtypes like TNBC or under metabolic stress, cancer cells might become overly reliant on exogenous carnitine transported by SLC22A5. In such a scenario, modulating its expression could disrupt a critical metabolic dependency, thereby inhibiting growth. Conversely, in ER+ tumors under stable conditions, SLC22A5 might primarily support anabolic growth. Our study, by identifying *SLC22A5* as a causal risk gene and a target of XHP, highlights its pharmacological relevance. However, the precise mechanistic outcome—whether inhibition or activation is therapeutic—likely depends on the intricate interplay of molecular subtype, tumor microenvironmental cues, and genetic background. Future work is warranted to delineate these conditions, which will be crucial for translating SLC22A5 into a precise therapeutic target. But currently, it is clear that SLC22A5 mutations can serve as a potential marker for the occurrence of breast cancer.

In this study, we first identified GSTM1 and SLC22A5 as two genes significantly negatively correlated with breast cancer risk through drug targets and Mendelian randomization. Subsequent in vitro experiments confirmed that silencing GSTM1 and SLC22A5 could promote the proliferation and migration of breast cancer cells, findings that were consistent with the outcomes of Mendelian randomization. The addition of XHP-containing serum was found to upregulate the

expression of GSTM1 and SLC22A5 in breast cancer cells. Concurrently, the proliferation and migratory capabilities of breast cancer cells cultured with XHP-containing serum were markedly inhibited. Our experimental results indicated that XHP has an inhibitory effect on the proliferation and migration of breast cancer, and its inhibitory effect may be exerted through these two genes, GSTM1 and SLC22A5. Our experimental results, along with previous reports, suggest that GSTM1 has a protective effect on breast cancer, which may be related to its participation in glutathione metabolism and antioxidation, thereby eliminating carcinogens in the body. However, whether XHP can affect the glutathione metabolic pathway to exert its tumor-suppressing effect still requires further research by our research group. Regarding SLC22A5, our experimental results seem to differ significantly from previous studies, but the association of SLC22A5 gene mutations with breast cancer risk is clear. In conclusion, our study discovered a new target for XHP in the treatment of breast cancer and verified its inhibitory effect on the proliferation and migration of breast tumor cells. This provides basic data support for the treatment of breast cancer with XHP, and at the same time, it offers a new direction for subsequent research and provides new ideas for precise treatment with traditional Chinese medicine. Finally, it is once again emphasized that the use of traditional Chinese medicine must be approved by medical authorities and can only be used as an adjunctive treatment, and must never replace the approved standard therapies.

Limitation

Currently, our study has several limitations. The network pharmacology analysis for target identification primarily relied on the TCMSP and SymMap databases. Although these are well-established and widely used resources, the exclusion of other specialized traditional Chinese medicine (TCM) databases—such as ETCM, HERB, and BATMAN-TCM—may have constrained the comprehensiveness of the initial target pool. Future studies should integrate multiple databases and adopt multi-omics approaches to construct a more comprehensive pharmacodynamic network of XHP, thereby providing a stronger foundation for causal inference and experimental validation. While our combined use of network pharmacology and Mendelian randomization (MR) leveraged large-scale genetic and transcriptomic data, it did not extend to other omics layers, such as proteomics or metabolomics. Incorporating such evidence would enhance the understanding of XHP's pharmacodynamic network and the post-transcriptional regulation of the identified targets. To date, we have conducted only phenotypic experiments without exploring the underlying molecular mechanisms in depth. Moreover, the absence of in vivo validation using animal models or clinical samples limits the physiological relevance and translational potential of our findings. Although we demonstrated that XHP upregulates GSTM1 and SLC22A5 and that silencing these genes promotes a malignant phenotype, the specific downstream signaling pathways through which these targets mediate their effects remain unclear. Further mechanistic studies are needed to delineate the precise molecular cascades involved. Addressing these limitations will be essential for translating our findings into clinically applicable strategies for precision TCM therapy in breast cancer. Our research group will continue to investigate the detailed molecular mechanisms by which XHP exerts its anti-breast cancer effects via GSTM1 and SLC22A5.

Conclusion

This study integrated network pharmacology and Mendelian randomization with in vitro experimental validation to systematically elucidate the potential mechanism of action of XHP against breast cancer. We successfully identified GSTM1 and SLC22A5 as two key target genes significantly negatively correlated with breast cancer risk. Our experiments demonstrated that inhibiting the expression of these two genes promoted the proliferation and migration of breast cancer cells; conversely, XHP-containing serum could up-regulate their expression and significantly inhibit the malignant phenotype of cancer cells. In conclusion, Xihuang Pill may exert its inhibitory effect on breast cancer progression by up-regulating the expression of GSTM1 and SLC22A5. Therefore, the GSTM1 and SLC22A5 targets identified and validated in this study not only provide novel insights into the anti-breast cancer mechanism of XHP but, more importantly, offer a crucial molecular foundation for the future development of biomarker detection and precision-guided adjuvant therapy strategies rooted in TCM.

Abbreviations

BC, breast cancer; TCM, traditional Chinese medicine; XHP, Xihuang Pill; GWAS, genome-wide association studies; MR, Mendelian randomization; SMR, summary-data-based Mendelian randomization; eQTL, expression quantitative trait locus; SNP, single nucleotide polymorphism; FDR, false discovery rate; HEIDI, heterogeneity in dependent instruments; OB, oral bioavailability; DL, drug-likeness; BCAC, Breast Cancer Association Consortium; siRNA, small interfering RNA; CCK-8, Cell Counting Kit-8; WB, Western blot; qRT-PCR, quantitative real-time polymerase chain reaction; cDNA, complementary DNA; FBS, fetal bovine serum; P/S, penicillin-streptomycin; EMT, epithelial-mesenchymal transition; TNBC, triple-negative breast cancer; ROS, reactive oxygen species; RAs, reactive aldehydes; OCTN2, organic cation/carnitine transporter 2; ER, estrogen receptor; IVW, inverse-variance weighted.

Acknowledgments

The authors thank the eQTLGen Consortium, the FinnGen study, and the Breast Cancer Association Consortium (BCAC) for making their summary data publicly available, which enabled the Mendelian randomization analyses in this study. We also acknowledge the valuable assistance of our laboratory members in data collection and experimental techniques. The funders had no role in the study design, data collection, analysis, manuscript preparation, or the decision to publish.

Funding

This work was supported by the National Natural Science Foundation of China (Grant No. 81973861), the Zhejiang provincial ministry medical and health Co-construction major project. (Grant No.2021435513), and Zhejiang Science and Technology Department “vanguard” “leading goose” research (Grant No. 2023C03044).

Disclosure

The authors declare that they have no conflict of interest.

References

1. Bray F, Laversanne M, Sung H, et al. Global cancer statistics 2022: GLOBOCAN estimates of incidence and mortality worldwide for 36 cancers in 185 countries. *CA Cancer J Clin*. 2024;74(3):229–263. doi:10.3322/caac.21834
2. Hong R, Xu B. Breast cancer: an up-to-date review and future perspectives. *Cancer Commun*. 2022;42(10):913–936. doi:10.1002/cac2.12358
3. Saha S, Mahapatra S, Khanra S, et al. Decoding breast cancer treatment resistance through genetic, epigenetic, and immune-regulatory mechanisms: from molecular insights to translational perspectives. *Cancer Drug Resist*. 2025;8:36. doi:10.20517/cdr.2025.69
4. Liu X, Gonzalez G, Dai X, et al. Adenylate kinase 4 modulates the resistance of breast cancer cells to tamoxifen through an m6A-based epitranscriptomic mechanism. *Mol Ther*. 2020;28(12):2593–2604. doi:10.1016/j.ymthe.2020.09.007
5. Ling Y, Liang G, Lin Q, et al. circCDYL2 promotes trastuzumab resistance via sustaining HER2 downstream signaling in breast cancer. *Mol Cancer*. 2022;21(1):8. doi:10.1186/s12943-021-01476-7
6. Tanwisa T, Raj A, Puttiga A, Gopinathan A, Alex AT. Role of MYC inhibition in overcoming resistance to HER2-targeted therapies for breast cancer. *Life Sci*. 2025;379:123902. doi:10.1016/j.lfs.2025.123902
7. Chen Z, Li Z, Yang S, Wei Y, An J. The prospect of Xihuang pill in the treatment of cancers. *Heliyon*. 2023;9(4):e15490. doi:10.1016/j.heliyon.2023.e15490
8. Xu X, Li X. The role of the xihuang pill in inhibiting triple-negative breast cancer through immunogenic cell death. *Breast Cancer*. 2025;17:793–803. doi:10.2147/BCTT.S545150
9. Xu H-B, Chen X-Z, Wang X, Pan J, Yi-Zhuo Z, Zhou C-H. Xihuang pill in the treatment of cancer: TCM theories, pharmacological activities, chemical compounds and clinical applications. *J Ethnopharmacol*. 2023;316:116699. doi:10.1016/j.jep.2023.116699
10. He H, Chen S. Research progress on the mechanism of action of Xihuang Pill in the treatment of breast cancer. *Chinese J Clin Oncol Rehabil*. 2025;32(1):25–31. doi:10.13455/j.cnki.cjcor.113494-20241210-0343
11. Li D, Fan H, Dong J, et al. Based on BATMAN-TCM to explore the molecular mechanism of xihuang pill regulating immune function to treat breast precancerous lesions. *Breast Cancer*. 2021;13:725. doi:10.2147/BCTT.S339607
12. Qi Z, Yan Z, Wang Y, et al. Integrative applications of network pharmacology and molecular docking: an herbal formula ameliorates H9c2 cells injury through pyroptosis. *J Ginseng Res*. 2023;47(2):228–236. doi:10.1016/j.jgr.2022.03.003
13. Li Z-Y, Dai Y-X, Wu Z-M, et al. Network pharmacology analysis and animal experiment validation of neuroinflammation inhibition by total ginsenoside in treating CSM. *Phytomedicine*. 2024;126:155073. doi:10.1016/j.phymed.2023.155073
14. Udrescu M, Ardelean SM, Udrescu L. The curse and blessing of abundance—the evolution of drug interaction databases and their impact on drug network analysis. *Gigascience*. 2022;12(1):giad011. doi:10.1093/gigascience/giad011
15. Emdin CA, Khera AV, Kathiresan S. Mendelian randomization. *JAMA*. 2017;318(19):1925–1926. doi:10.1001/jama.2017.17219
16. Schmidt AF, Finan C, Gordillo-Marañón M, et al. Genetic drug target validation using Mendelian randomisation. *Nat Commun*. 2020;11(1):3255. doi:10.1038/s41467-020-16969-0

17. Kreitmaier P, Katsoula G, Zeggini E. Insights from multi-omics integration in complex disease primary tissues. *Trends Genet*. 2023;39(1):46–58. doi:10.1016/j.tig.2022.08.005
18. Sun X, Chen B, Qi Y, et al. Multi-omics Mendelian randomization integrating GWAS, eQTL and pQTL data revealed GSTM4 as a potential drug target for migraine. *J Headache Pain*. 2024;25(1):117. doi:10.1186/s10194-024-01828-w
19. Höller A, Nguyen-Sträuli BD, Frauchiger-Heuer H, Ring A. "Diagnostic and prognostic biomarkers of luminal breast cancer: where are we now?" *Breast Cancer*. 2023;15:525–540. doi:10.2147/BCTT.S340741
20. Y F, D S, L Y, et al. Advancements in clinical aspects of targeted therapy and immunotherapy in breast cancer. *Molecular Cancer*. 2023;22(1). doi:10.1186/s12943-023-01805-y
21. Ru J, Li P, Wang J, et al. TCMSP: a database of systems pharmacology for drug discovery from herbal medicines. *J Cheminform*. 2014;6(1):13. doi:10.1186/1758-2946-6-13
22. Wu Y, Zhang F, Yang K, et al. SymMap: an integrative database of traditional Chinese medicine enhanced by symptom mapping. *Nucleic Acids Res*. 2019;47(D1):D1110–D1117. doi:10.1093/nar/gky1021
23. Liu S, Zhou X, Zhang L, Luo W. Network pharmacology and bioinformatics approach to unravel the mechanism of Xiao-chai-hu-tang herbal formula in tinnitus treatment. *Heliyon*. 2024;10(18):e37584. doi:10.1016/j.heliyon.2024.e37584
24. Ren Y, Nie L, Zhu S, Zhang X. Nanovesicles-mediated drug delivery for oral bioavailability enhancement. *Int J Nanomedicine*. 2022;17:4861–4877. doi:10.2147/IJN.S382192
25. Jia C-Y, Li J-Y, Hao G-F, Yang G-F. A drug-likeness toolbox facilitates ADMET study in drug discovery. *Drug Discov Today*. 2020;25(1):248–258. doi:10.1016/j.drudis.2019.10.014
26. Bateman A, Martin M-J, Orchard S, UniProt Consortium. UniProt: the universal protein knowledgebase in 2025. *Nucleic Acids Res*. 2025;53(D1): D609–D617. doi:10.1093/nar/gkae1010
27. Võsa U, Claringbould A, Westra H-J, et al. Large-scale cis- and trans-eQTL analyses identify thousands of genetic loci and polygenic scores that regulate blood gene expression. *Nat Genet*. 2021;53(9):1300–1310. doi:10.1038/s41588-021-00913-z
28. Kurki MI, Karjalainen J, Palta P, et al. FinnGen provides genetic insights from a well-phenotyped isolated population. *Nature*. 2023;613 (7944):508–518. doi:10.1038/s41586-022-05473-8
29. Zhu Z, Zhang F, Hu H, et al. Integration of summary data from GWAS and eQTL studies predicts complex trait gene targets. *Nat Genet*. 2016;48 (5):481–487. doi:10.1038/ng.3538
30. Jiang P, Zhao Y, Jia Y, et al. Multi-omics study on autophagic dysfunction molecular network in the pathogenesis of rheumatoid arthritis. *J Transl Med*. 2025;23(1):274. doi:10.1186/s12967-025-06288-7
31. Sun Y, Liu Y, Dian Y, Zeng F, Deng G, Lei S. Association of glucagon-like peptide-1 receptor agonists with risk of cancers-evidence from a drug target Mendelian randomization and clinical trials. *Int J Surg*. 2024;110(8):4688–4694. doi:10.1097/JS9.0000000000001514
32. Michailidou K, Lindström S, Dennis J, et al. Association analysis identifies 65 new breast cancer risk loci. *Nature*. 2017;551(7678):92–94. doi:10.1038/nature24284
33. Liu J, Wang S, Zhang Y, Fan H-T, Lin H-S. Traditional C hinese medicine and cancer: history, present situation, and development. *Thorac Cancer*. 2015;6(5):561–569. doi:10.1111/1759-7714.12270
34. Luo S, Huang Z, Dai Y, et al. Xihuang pill suppressed primary liver cancer growth by downregulation of AFP and YAP signaling. *J Ethnopharmacol*. 2025;348:119891. doi:10.1016/j.jep.2025.119891
35. Zhuang Z, Huang D, Sheng ZR, et al. Systems biology strategy and experimental validation to uncover the pharmacological mechanism of Xihuang Pill in treating non-small cell lung cancer. *Phytomedicine*. 2023;108:154491. doi:10.1016/j.phymed.2022.154491
36. Wang Y, Wang W, Liu K, et al. The mechanism of Xihuang pills' intervention in the tumour immune microenvironment for the treatment of liver cancer based on the STAT3-PDL1 pathway. *J Ethnopharmacol*. 2024;331:118278. doi:10.1016/j.jep.2024.118278
37. Hong W, Tang H, Wang D, et al. Xihuang pill suppresses breast cancer malignancy by inhibiting TGF-β signaling and acquires chemotherapy benefits. *J Ethnopharmacol*. 2025;337(Pt 3):119000. doi:10.1016/j.jep.2024.119000
38. Yang H, Bi Y, Wang M, Liu Y, Naseem A, Huang J. Xihuang pill suppresses triple-negative breast cancer via regulating AXL/TGF-β1/RhoA/ ROCK and ERK pathway. *J Ethnopharmacol*. 2025;344:119556. doi:10.1016/j.jep.2025.119556
39. Qiu Y, Zhang G, Su R, et al. Mechanism of Xihuang pill inhibition of SLC7A11 deubiquitination through downregulation of the OTUB1 to promote ferroptosis in triple-negative breast cancer. *J Ethnopharmacol*. 2025;353:120456. doi:10.1016/j.jep.2025.120456
40. Levy R, Le TH. Role of GSTM1 in hypertension, CKD, and related diseases across the life span. *Kidney360*. 2022;3(12):2153–2163. doi:10.34067/ KID.0004552022
41. Singh SP, Dhanasekara CS, Melkus MW, et al. Relevance of cellular homeostasis-related gene expression signatures in distinct molecular subtypes of breast cancer. *Biomedicines*. 2025;13(5):1058. doi:10.3390/biomedicines13051058
42. Ho E, Wong CP, Bouranis JA, Shannon J, Zhang Z. Cruciferous vegetables, bioactive metabolites, and microbiome for breast cancer prevention. *Annu Rev Nutr*. 2025;45(1):171–195. doi:10.1146/annurev-nutr-062222-024321
43. Zheng S, Yan J, Wang J, et al. Unveiling the effects of cruciferous vegetable intake on different cancers: a systematic review and dose-response meta-analysis. *Nutr Rev*. 2025;83(5):842–858. doi:10.1093/nutrit/nuae131
44. Yu Y, Zhang Z, Dong X, et al. Pangenomic analysis of Chinese gastric cancer. *Nat Commun*. 2022;13(1):5412. doi:10.1038/s41467-022-33073-7
45. Larsson SC, Chen J, Ruan X, Li X, Yuan S. Genome-wide association study and Mendelian randomization analyses reveal insights into bladder cancer etiology. *JNCI Cancer Spectrum*. 2025;9(2):pkaf014. doi:10.1093/jncics/pkaf014
46. Nigam SK. The SLC22 transporter family: a paradigm for the impact of drug transporters on metabolic pathways, signaling, and disease. *Annu Rev Pharmacol Toxicol*. 2018;58(1):663–687. doi:10.1146/annurev-pharmtox-010617-052713
47. Gründemann D. The ergothioneine transporter controls and indicates ergothioneine activity — a review. *Prev Med*. 2012;54:S71–74. doi:10.1016/j. ypmed.2011.12.001
48. Jong NN, Nakanishi T, Liu JJ, Tamai I, McKeage MJ. Oxaliplatin transport mediated by organic cation/carnitine transporters OCTN1 and OCTN2 in overexpressing human embryonic kidney 293 cells and rat dorsal root ganglion neurons. *J Pharmacol Exp Ther*. 2011;338(2):537–547. doi:10.1124/jpet.111.181297
49. Hu S, Franke RM, Filipski KK, et al. Interaction of imatinib with human organic ion carriers. *Clin Cancer Res*. 2008;14(10):3141–3148. doi:10.1158/1078-0432.CCR-07-4913

50. Kou L, Hou Y, Yao Q, et al. L-Carnitine-conjugated nanoparticles to promote permeation across blood-brain barrier and to target glioma cells for drug delivery via the novel organic cation/carnitine transporter OCTN2. *Artif Cells Nanomed Biotechnol*. 2018;46(8):1605–1616. doi:10.1080/21691401.2017.1384385
51. Wang C, Uray IP, Mazumdar A, Mayer JA, Brown PH. SLC22A5/OCTN2 expression in breast cancer is induced by estrogen via a novel intronic estrogen-response element (ERE). *Breast Cancer Res Treat*. 2012;134(1):101–115. doi:10.1007/s10549-011-1925-0
52. Lee J-H, Zhao X-M, Yoon I, et al. Integrative analysis of mutational and transcriptional profiles reveals driver mutations of metastatic breast cancers. *Cell Discov*. 2016;2(1):16025. doi:10.1038/celldisc.2016.25